

# Synthesis of mesoporous TiO<sub>2</sub> template-free and photocatalytic activity for azo dye degradation

Sawsan A. Mahmoud<sup>1\*</sup> Agnes Szegedi<sup>2</sup> Ahmed K. Aboul Gheit<sup>1</sup>

1. Processes Development Department, Egyptian Petroleum Research Institute, PO box 11727, 1, Ahmed El-Zomor St., Nasr City, Cairo, Egypt.
2. Research Centre for Natural Sciences, Hungarian Academy of Sciences, Pusztaszeri út 59-67, 1025 Budapest, Hungary.

\* E-mail of the corresponding author: [sawsanhassan2003@yahoo.com](mailto:sawsanhassan2003@yahoo.com)

## Abstract

Nanoporous titanium dioxide was prepared by sol-gel technique. To control the surface area, pore size and pore volume of the prepared TiO<sub>2</sub>, a catalyzed hydrolysis was carried out using different concentrations of silicotungstic acid (SWA) as a template. A fixed molar ratio of H<sub>2</sub>O/Ti was used. The prepared TiO<sub>2</sub> was calcined at 400 or 600°C. Samples were characterized by nitrogen physisorption, X-ray powder diffraction (XRD), selected scattered electron diffraction, scanning and transmission electron microscopy (SEM and TEM). The photocatalytic activity of the prepared samples was evaluated by the degradation of alizarin yellow under UV light. The results showed that the crystallinity increases as the concentration of SWA decreases. The presence of SWA during the precipitation of TiO<sub>2</sub> prevents the formation of rutile phase and suppresses the crystal growth. The results showed also that the surface area increases as the concentration of SWA decreases. The samples prepared using 0.05M SWA and calcined at 600 °C showed a higher activity.

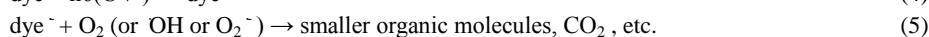
**Keywords:** mesoporous TiO<sub>2</sub>, photocatalytic degradation, alizarin yellow, azodye.

## 1. Introduction

The dyeing wastewaters discharge a large number of hazardous pollutants, in which, the percentage of azo dyes accounts for about 70% of all dyestuffs by weight (Singh & Arora 2011). Azo dyes and their intermediates, e.g., aromatic amines, are toxic, carcinogenic and mutagenic, which may pose a potential health hazard to humans (Turesky 2005; Dumont *et al.* 2010). Nowadays, the dyeing wastewaters are mostly treated by biological processes. However, the biological degradation of azo dye is difficult. Furthermore, azo dye could inhibit the microbial activity and cause cell death at high concentration. Moreover, the effluent of biological treatment of dyeing wastewater was proved to be carcinogenic and mutagenic (Lima *et al.* 2007). To improve the biodegradability of azo dyeing wastewaters, combining advanced oxidation processes (AOPs) with biological process was pursued in recent years (Wang & Xu 2012). AOPs, defined as those technologies that utilize the hydroxyl radical (OH) for oxidation, including ozonation (Fu *et al.* 2011), Fenton oxidation (Tantak & Chaudhari 2006; Lodha & Chaudhari 2007), electrochemical oxidation (Guo 2006), or UV/H<sub>2</sub>O<sub>2</sub> (Sudarjanto *et al.* 2006), followed by aerobic process are efficient for azo dyes degradation. Ionizing radiation (e.g., gamma radiation or electron beam) is a special kind of AOP (Sudarjanto *et al.* 2006), which can produce approximately equal amounts of oxidizing species (d<sub>OH</sub> and H<sub>2</sub>O<sub>2</sub>) and reducing species (e<sub>aq</sub><sup>-</sup> and H<sub>2</sub>) through water radiolysis. This technology has been receiving more and more attention for removal and/or pretreatment of azo dyes and other toxic pollutants (Jianlong & Jiazhao 2007; Sharma *et al.* 2003; Hu & Wang 2007; Ting & Jamaludin 2008; Wojnarovits & Takacs 2008; Vahdat 2010; Yu *et al.* 2010) but this technology is more expensive than chlorine or ultraviolet disinfection. Because of this gamma irradiation is unlikely to be applied.

Photocatalytic degradation and mineralization of organic and inorganic pollutants by means of semiconductor TiO<sub>2</sub> have been extensively studied in order to solve environmental problems relating to waste waters and polluted air (Hoffmann *et al.* 1995; Hogfelt & Gratzel 1995; Fox & Dulay 1993; Pelizzetti & Serpone 1989; Heller 1995; Anpo & Yamashita 1996; Kamat 1993; Ollis & Al-Ekabi 1993). Among various metal oxide semiconductors, TiO<sub>2</sub> has been in the focus of photocatalysis under UV irradiation because of its physical and chemical stability, low cost, ease of availability, non-toxicity and electronic and optical properties.

Azo-dyes are abundant class of synthetic, colored, organic compounds, characterized by the presence of one or more azo bonds (-N=N-). Synthetic textile dyes of the azo family represent an important part of the world production of synthetic dyes. They are degraded into potentially carcinogenic amines (Chung & Stevens 1993; Nerud *et al.* 2001). Moreover, their color causes an aesthetic problem in receiving waters. The degradation mechanism of dye using TiO<sub>2</sub> can be described by the following steps:



Nowadays, progress is focusing on to prepare anatase TiO<sub>2</sub> phase of high surface area and controlled pore size, aiming to enhance the charge transfer efficiency. Generation of these highly controlled materials can be achieved by combining sol-gel techniques with the evaporation process taking place in the presence of a surfactant templating agent (Soler-Illia *et al.* 2002; Soler-Illia *et al.* 2003). After elimination of the organic template and controlled crystallization of the network (Grosso *et al.* 2003), one ends up with an organized arrangement of anatase nanoparticles shaped in mesoporous framework with narrow pore size distribution adjusted by the conditions and the surfactant molecular weight (Sakatani *et al.* 2006). Previous studies published in the literature emphasize the preparation of mesoporous TiO<sub>2</sub> without using template as reported by (Li *et al.*, 2012, 2013), (Liu *et al.*, 2012), (Gao *et al.*, 2014) and (Abdel-Azim *et al.*, 2014). Other published literatures emphasize the preparation of mesoporous TiO<sub>2</sub> using different templates such reported by (Chevallier *et al.*, 2012), (Bawer *et al.*, 2012), (Zhao *et al.*, 2012), (Duan *et al.*, 2013), (Zhou *et al.*, 2014), (Park *et al.*, 2014), (Kim *et al.*, 2013), (Xiong *et al.*, 2011), (Di *et al.*, 2006), (Faisal *et al.*, 2014), (Wang *et al.*, 2013) and (Qiona *et al.*, 2013). Other researchers used mixed template during the preparation of mesoporous TiO<sub>2</sub> as (Wang *et al.*, 2014), (Onsuratoom *et al.*, 2011), (Jantawasu *et al.*, 2009) and (Sreethawong *et al.*, 2005).

Generally, a sol-gel method based on the hydrolysis of titanium alkoxide is widely used to synthesize TiO<sub>2</sub> nanoparticles (Lakshmi *et al.* 1997). However, this method encounters some problems, such as weak anatase crystallinity and poor monodispersity. In addition, nanocrystalline TiO<sub>2</sub> prepared by the sol-gel method undergoes both phase transformation and crystallite size growth even at relative low temperature (Zhang *et al.* 2006). To apply TiO<sub>2</sub> particles synthesized from the sol-gel process as photocatalytic catalysts, it is important to maintain high anatase crystallinity (Cao *et al.* 2011). A previous study reported that high degree of anatase crystallinity can be achieved without high temperature calcination when TiO<sub>2</sub> particles were synthesized at low temperature due to fast hydrolysis and slow condensation (Nikkanen *et al.* 2007). In addition, many studies regarding the evaluation of the photocatalytic activity of TiO<sub>2</sub> nanoparticles have been conducted (Fujishima *et al.* 2000; Chong *et al.* 2010; Yu *et al.* 2007); however, few focused on the correlation between parameters used in the synthesis process of TiO<sub>2</sub> nanoparticles and their photocatalytic activity (Chong *et al.* 2010; Yu *et al.* 2007; Li *et al.* 2006).

Therefore, in this study we pay attention to the effect of the synthesis condition using silicotungstic acid in different concentration as a template on the physical properties of mesoporous TiO<sub>2</sub>, in particular on its crystal composition, thermal stability, pore size distribution, surface area, and photocatalytic activity. The prepared materials were calcined at various temperatures and their crystalline composition, thermal stability, pore size distribution, surface area and photocatalytic activity were compared.

## 2. Experimental

### 2.1. Materials

Titanium (IV) isopropoxide, silicotungstic acid H<sub>4</sub>[W<sub>12</sub>SiO<sub>40</sub>] and the absolute ethanol were provided from Sigma-Aldrich CO.USA. The analytical grade alizarin yellow C<sub>13</sub>H<sub>9</sub>N<sub>3</sub>O<sub>5</sub> was used without further purification.

### 2.2. Preparation of titanium dioxide

Titanium dioxide was prepared using sol-gel method as follows: 3.6 g of titanium tetraisopropoxide was diluted by absolute ethanol with constant stirring in a weight ratio of 1/7. After 15 min, 0.48 ml of silicotungstic acid (SWA) was added. The resulting suspension was stirred for three hours at room temperature, followed by the addition of 26 moles of waters per mole of Ti with vigorous stirring for two hours followed by the evaporation of water and ethanol at 78 °C. The resulting precipitate was washed with deionized water and ethanol, drying under vacuum at 80 °C overnight, and then calcined at 400 or 600 °C for three hours.

### 2.3. Characterization of TiO<sub>2</sub>

Nitrogen physisorption isotherms were measured at -196 °C using Quantachrome Nova Win 2 apparatus. The average pore size and pore size distribution were calculated using the Barrett-Joyner-Halenda (BJH) method from the desorption branch of the isotherms.

Crystalline phase of the TiO<sub>2</sub> formed was determined applying a Philips RB diffractometer in reflection mode using MoK $\alpha$  radiation at 40 kV, 40 mA.

The crystalline phases of TiO<sub>2</sub> were also investigated by scattered electron diffraction using a MORGAGNI 268D type (100 kV; W filament; point-resolution = 0.5 nm).

Surface morphology of the prepared TiO<sub>2</sub> was performed on JEOL JEM 3500 electron microscope.

Transmission electron microscopy (TEM) studies were carried out using a JEOL JEM-1230 electron microscope operating at 120 kV.

The pore structure of TiO<sub>2</sub> was investigated by a MORGAGNI 268D type (100 kV; W filament; point-resolution = 0.5 nm) scanning electron microscope.

### 2.4. Photodegradation of Alizarin yellow

500 ccm of an aqueous solution containing 10 ppm of high purity Alizarin yellow was subjected to UV irradiation using a 6 watt lamp at a wavelength of 254 nm. All photodegradation experiments were conducted in a batch reactor. The UV lamp was placed in a cooling silica jacket and placed in a jar containing the polluted water. The catalyst (0.05 g) was stirred in the

solution using a magnetic stirrer at a controlled reaction temperature of 25 °C during the experimental period. At different irradiation time intervals, samples of the irradiated water were withdrawn for analysis and the dye concentration was determined by absorption mode (using calibration curve of absorbance & the concentration of the dye) 8500 series UV-Visible spectrophotometer.

### 3. RESULTS AND DISCUSSION

#### 3.1. Effect of SWA concentration and calcination temperature on the physicochemical structure of TiO<sub>2</sub>

Figure 1 (a&b) shows the nitrogen adsorption-desorption isotherms, and the pore size distribution of a TiO<sub>2</sub> sample calcined at 400°C. The isotherms are of type IV with H2 type hysteresis loop classified by IUPAC (IUPAC reporting physisorption data for gas/solid system 1985) with closure point ranging between p/p<sub>0</sub>=0.3-0.4 and a quite steep condensation step indicating the mesoporous nature of the solid. The H2 type hysteresis loop is generally attributed to pores of narrow entrance and wider body, i.e. ink bottle like shape. The amount of adsorbed nitrogen increases simultaneously with decreasing in SWA content indicating increasing adsorption capacity of the samples. The decrease in surface area with increasing SWA content can be attributed to a lower cross-linking degree during the sol-gel synthesis process (Phonthammachat *et al.* 2003; Khalil *et al.* 1998). These features are reflected in surface parameters, pore volume and average pore radius especially for the samples embedded low SWA content. Figure 2/a&b also shows the widening of the hysteresis loop which is more pronounced after introduction of SWA, and increases with decreasing SWA content implying the successful role of SWA in creating mesoporous system. It should be emphasized that the surface parameters are related to SWA content and the crystalline features of the samples (Table 1). Figure 2/a shows the pore size distribution for the calcined samples at 400°C. It is obvious that as the SWA increases bimodal pores are formed. This indicates highly incorporated SWA in the TiO<sub>2</sub> structure.

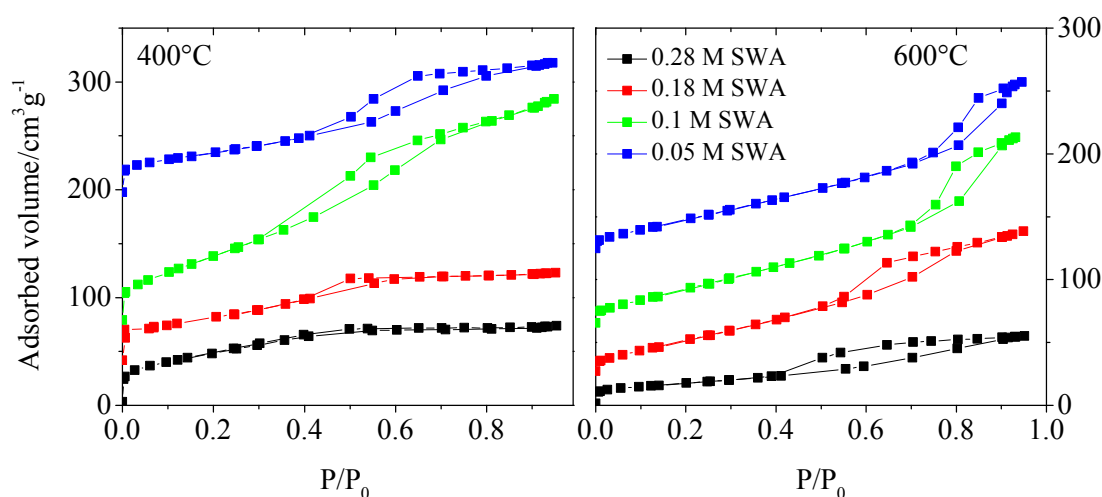


**Figure 1:**  
 Nitrogen physisorption isotherms for TiO<sub>2</sub> prepared by different concentrations of SWA calcined at 400 °C and 600 °C for 3 h.

**Table 1**

Textural properties of TiO<sub>2</sub> calcined at 400 °C using different concentrations of SWA.

SWA conc. (Mol/L)	BET surface area (m <sup>2</sup> /g)	Total pore volume (cm <sup>3</sup> /g)	Average pore diameter (nm)	Crystallite size (nm)
0.28	140.0	0.11	10.9	18.2
0.18	153.0	0.12	18.2	15.0
0.1	173.7	0.18	18.1	12.1
0.05	256.6	0.31	21.6	9.1
Ref. a	93	0.10	5.8	-

<sup>a</sup>Mesoporous TiO<sub>2</sub> was prepared using phosphotungstic acid assisted hydrolysis and polycondensation reactions of tetrabutyl titanate, followed by removal of the template via washing with water and ethanol. Luo, G.S. *et al.* (2006), *Microporous and*

The experimental results show that the surface area is influenced by the annealing temperature, whereas the mesopore size and the total pore volume are influenced by the amount of SWA and the annealing temperature (Table 2). The average mesopore diameter and the total pore volume decrease with increasing the concentration of SWA. Increasing the calcination temperature the surface area and the total pore volume are decreasing rapidly due to the growth of the crystallite size (Figure 2 a&b).

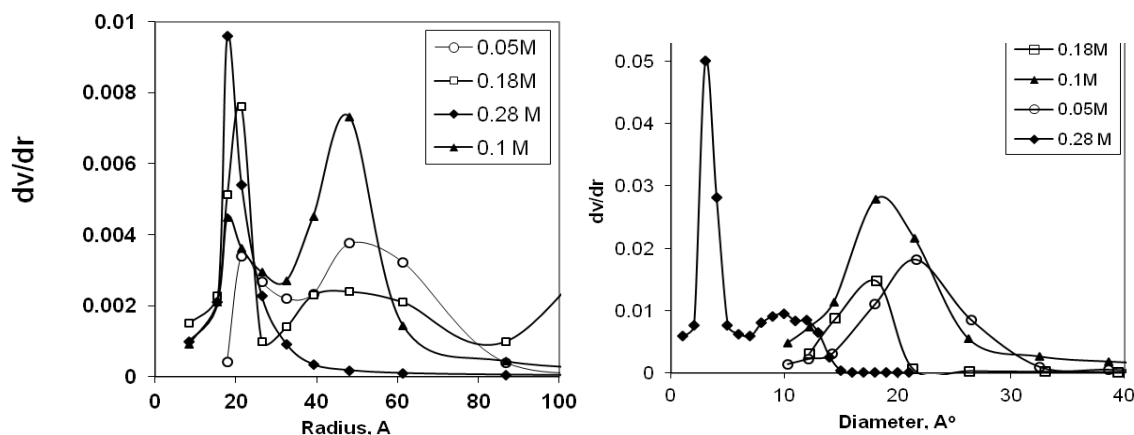


**Figure 2**  
 Pore size distribution for TiO<sub>2</sub> prepared by different amounts of SWA, calcined at (a): 400°C and (b) 600°C

**Table 2**

Textural properties of TiO<sub>2</sub> calcined at 600 °C using different concentrations of SWA.

SWA conc. (Mol/L)	BET surface area (m <sup>2</sup> /g)	Total pore volume (cm <sup>3</sup> /g)	Average pore diameter (nm)	Crystallite size (nm)
0.28	61.9	0.08	3.6	24.5
0.18	107.0	0.17	4.3	18.3
0.1	102.0	0.21	9.7	14.3
0.05	132.9	0.23	9.7	11.5

The X-ray diffraction (XRD) patterns of the calcined TiO<sub>2</sub> material prepared under various concentrations of SWA calcined at 400°C and 600°C are shown in Figure 3 a&b. All the reflections can be assigned to anatase phase without any indication the presence of any crystalline SWA. Hence, SWA was successfully incorporated into TiO<sub>2</sub> structure, rather than existing as a free solid acid. The peak found at 11.5 °2θ is the most intensive peak for the anatase phase. This peak is relatively broad due to the nano-sized dimension of the crystals. The particle sizes estimated by the Sherrer equation are varying between 9-18 nm, depending on the SWA concentration for samples calcined at 400°C and between 12-36 nm for samples calcined at 600°C. It should be emphasized that SWA plays a vital role in controlling the particle growth and the nature of crystalline phases. The addition of small amount of SWA is considered as a prime factor in stabilizing the anatase phase and hinders its transformation to the more stable rutile phase. Anatase appears to be the most photocatalytically and electrochemically active crystallographic form of TiO<sub>2</sub>, opposed to the rutile and brookite forms; herein, the prepared mesoporous TiO<sub>2</sub> materials may have far-reaching implications for its use as a photocatalytic material.

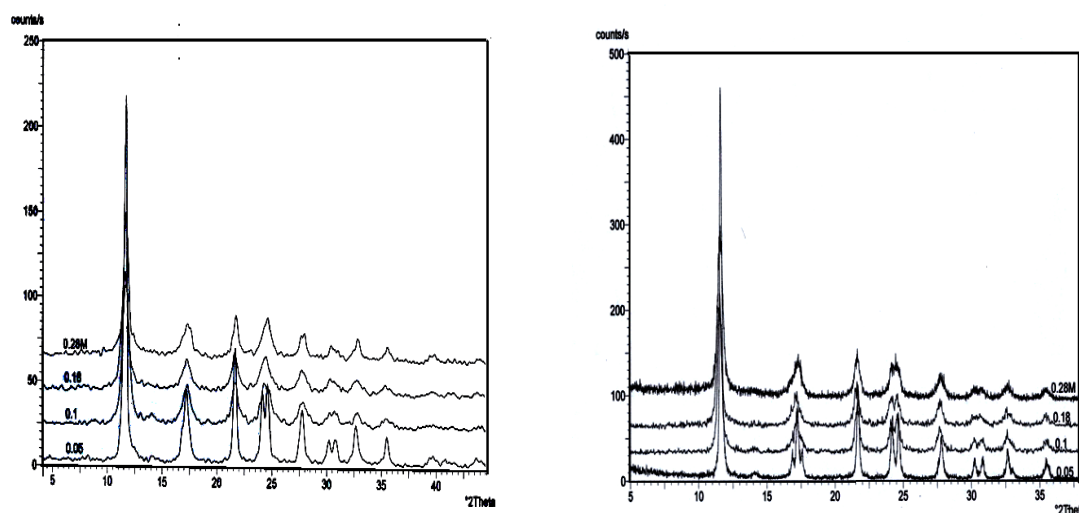


**Figure 3**

**XRD patterns of TiO<sub>2</sub> prepared using different SWA concentrations, calcined at (a): 400°C and (b) 600°C for 3 h.**

Selected area scattered electron diffraction (Figure 4) also supported that with increasing temperature the crystallinity of the anatase phase also increases. It is also obvious that the anatase crystallinity increases as the SWA content increases.

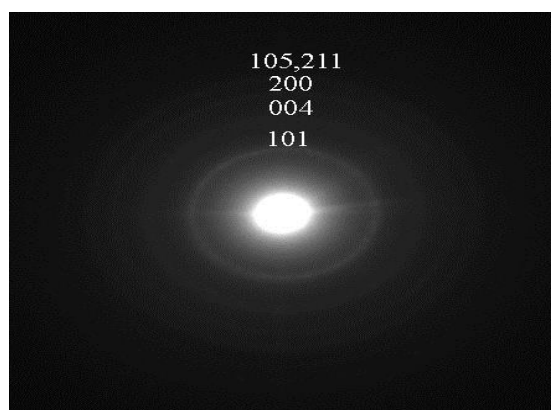


**Figure 4**

**Electron diffraction pattern for TiO<sub>2</sub> prepared using 0.1 M SWA, heat treated at 600 °C.**

Surface morphology of the prepared TiO<sub>2</sub> samples calcined at 400 and 600°C are presented in Figure 5. The SEM images show that TiO<sub>2</sub> particles have well-defined spherical morphology, with a diameter range of 7–8 μm.

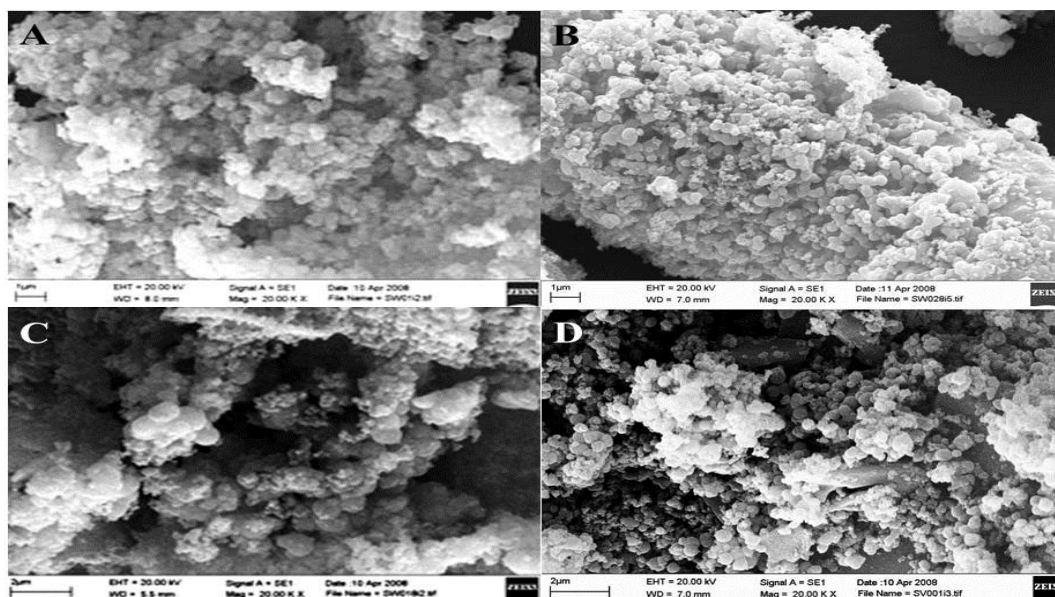


**Figure 5**  
SEM images for  $\text{TiO}_2$  prepared by different SWA concentrations: a) 0.28 M, b) 0.18 M, c) 0.1 M and d) 0.05 M and calcined at 400 °C for 3 h.

TEM images in Figure 6 show the aggregation of nanoparticles with particle size of 11-24 nm. A disordered wormhole-like pore structure can be observed, which is formed by the agglomeration of  $\text{TiO}_2$  nanoparticles. The accessible pores are randomly connected, lacking discernible long-range order in the pore arrangement among the small  $\text{TiO}_2$  particles. This indicates that the mesoporosity is mainly due to the inter-particle porosity rather than intra-particle porosity.

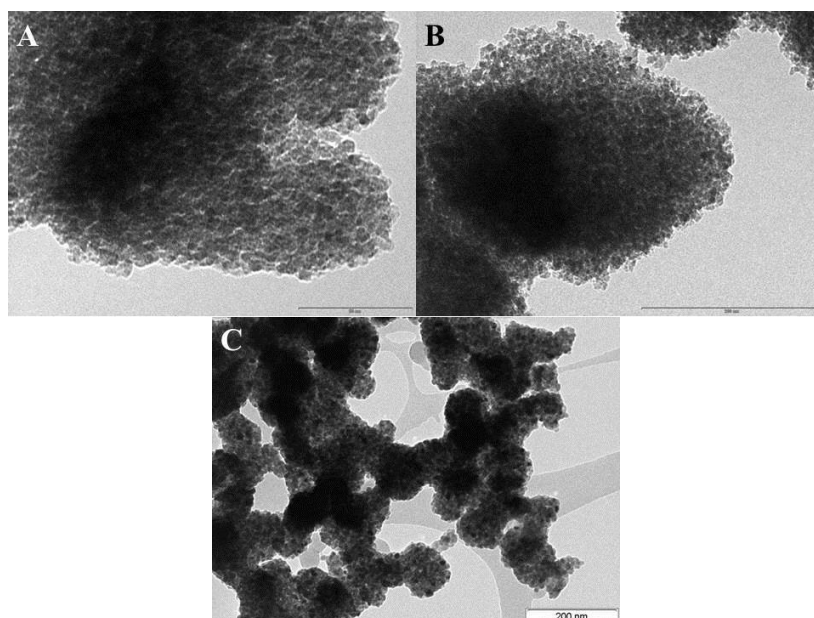


**Figure 6:**  
TEM images for  $\text{TiO}_2$  prepared by different SWA concentrations: a) 0.1 M, b) 0.05 M and c) 0.28 M and calcined at 600 °C for 3 h.

### 3.2. Mechanism of Formation Mesoporous $\text{TiO}_2$

A possible mechanism for the formation of well-dispersed mesoporous  $\text{TiO}_2$  particles might be effective aggregation of the

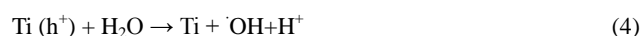
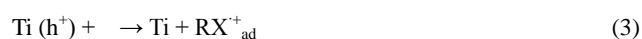
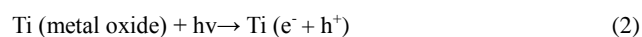
TiO<sub>2</sub> particles in the presence of SWA. The SWA plays an important role in the formation of a stable sol–gel network with ordered array of Ti and O, without leading to the shrinkage and collapse of the network. The basic unit of SWA is the heteropolyanion of Keggin structure H<sub>4</sub>[W<sub>12</sub>SiO<sub>40</sub>], which is the most commonly studied heteropolyanions because of its great acid strength, stability, and availability compared to those of other polyoxometalates. A Keggin unit of SWA (Janik *et al.* 2003) is composed of a central SiO<sub>4</sub> tetrahedron surrounded by twelve WO<sub>6</sub> octahedra. There are four types of oxygen atoms in the Keggin unit: four oxygen atoms of the central tetrahedron, 12 oxygen atoms that bridge addenda atoms not sharing a central oxygen atom (corner-sharing), 12 oxygen atoms that bridge two addenda atoms sharing the same central oxygen atom (edge-sharing), and twelve terminal oxygen atoms associated with a single addendum atom (Janik *et al.* 2005). A hydrogen bond is easily formed between the proton on the Keggin unit and the oxygen atom of the water molecule. Bidentate water adsorption includes formation of a second hydrogen bond between a hydrogen atom of the water molecule and a second oxygen atom of the Keggin unit. Hydrogen bonds between SWA and hydroxylated tetrabutyl titanate are the essential factor to form this mesoporous structure. It is reported that mesoporous silica could be prepared by the hydrogen-bonding interaction of an alkylamine (S0) head group and hydroxylated TEOS (I0) (Tanev & Pinnavaia 1995). Similarly, surfactants with head groups that could interact with the titanium alkoxide will lead to TiO<sub>2</sub> mesostructures. This indicates that, without the formation of ordered micelles by hydrophilic and hydrophobic surfactants, SWA can be used successfully as a self-assembling template via formation of hydrogen bonds. Consequently, the titanium precursor is hydrolyzed and condensed around the self-assembled PWA structure combined with water at a controlled rate, resulting in the formation of highly porous crystalline TiO<sub>2</sub>. The materials lack long-range ordering of pores and have higher amounts of interparticle mesoporosity, because the long-range effects of the electrostatic interaction that could control the packing of micellar rods are absent.

### 3.3. Photocatalytic degradation of Alizarin yellow

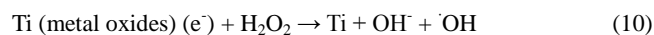
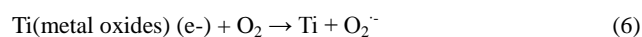
Titanium dioxide is considered as a promising photocatalyst extensively involved in partial or complete mineralization of various hazardous organic dyes through the active species on its surface. Once titanium dioxide is illuminated with UV light, electrons are excited from the lower energy valence band to the conducting band, which leads to the formation of positive holes and negative electrons on the catalyst surface. The holes react with water or hydroxyl ions producing hydroxyl radicals. Electrons in the conduction band (e<sub>CB</sub><sup>-</sup>) on the catalyst surface can reduce molecular oxygen to a superoxide anion. Hydroxyl (HO<sup>•</sup>), hydrogen peroxide (HO<sub>2</sub><sup>•</sup>), and superoxide (O<sub>2</sub><sup>•-</sup>) radicals are considered the reactive species that oxidize the organic compounds adsorbed on the oxide surface (Hoffmann *et al.* 1995).

These generated radicals are usually react with the adsorbed dye molecules followed by the formation of several intermediates including radicals, and radical cations finally mineralized into carbon dioxide, water and inorganic nitrogen from nitrate ion.

The response mechanism of the electrons and holes of the Ti catalyst is expressed as follows:



The electrons will, therefore, be transmitted via substances absorbed on the surface of the Ti catalyst such as H<sub>2</sub>O, dye, and <sup>•</sup>OH. In addition, Organic compounds absorbed on the surface of Ti catalyst then oxidized by <sup>•</sup>OH.



The photocatalytic activity of the prepared samples was determined by degradation of x M alizarin yellow solution under UV-light irradiation (Figure 7 a&b). For 0.28 M SWA sample no degradation of alizarin yellow was observed over a long period (180 min). For 0.18M SWA sample already a low degradation activity can be found. As the concentration of SWA decreases the photocatalytic activity increases to reach 100% after 180 min using 0.05M SWA. The photoactivity of TiO<sub>2</sub> in degradation process is influenced by several parameters such as the phase composition, band-gap energy, surface area, particle size, crystallinity and electron hole recombination rate (Boujday *et al.* 2004; Zhang *et al.* 2005; Ding *et al.* 2000). different Azo Dyes photodegradation were studied by several research groups; (Topkaya *et al.* 2014; Guo *et al.* ; Shariffuddin *et al.* 2013; Kalasin *et al.* 2011; Nešić *et al.*, 2013 ; Luc'ic' *et al.* 2014; Ilinoiu *et al.* 2013; Narayanasamy & Murugesan 2014; Jiao *et al.* 2014). High surface area mesoporous titania is considered a reactive photocatalyst in degradation process owing to the facility of alizarin yellow dye molecules to adsorb on the various active surface centers and its ability to diffuse through the large pore structure (Gopal *et al.* 1997; Lv *et al.* 2011; Han *et al.* 2012). Fig.10b represents the photocatalytic degradation of the prepared catalyst calcined at 600°C. The same trend can be observed as for samples annealed at 400 °C but with higher activity. 100% degradation was obtained in 120 min using 0.05 M SWA. (Han *et al.* 2012; Tian *et al.* 2009) reported that, if specific surface area and pore volume of TiO<sub>2</sub> nanoparticles were dominant factors controlling the photocatalytic activity of TiO<sub>2</sub>, the activity would have decreased with calcination temperature; however, the activity showed the maximum value at 700 °C in his study. The trend is likely attributed to the combined effect of anatase crystallinity which showed the highest value at 600 °C, and to crystallite size which did not excessively increased up to 600 °C.

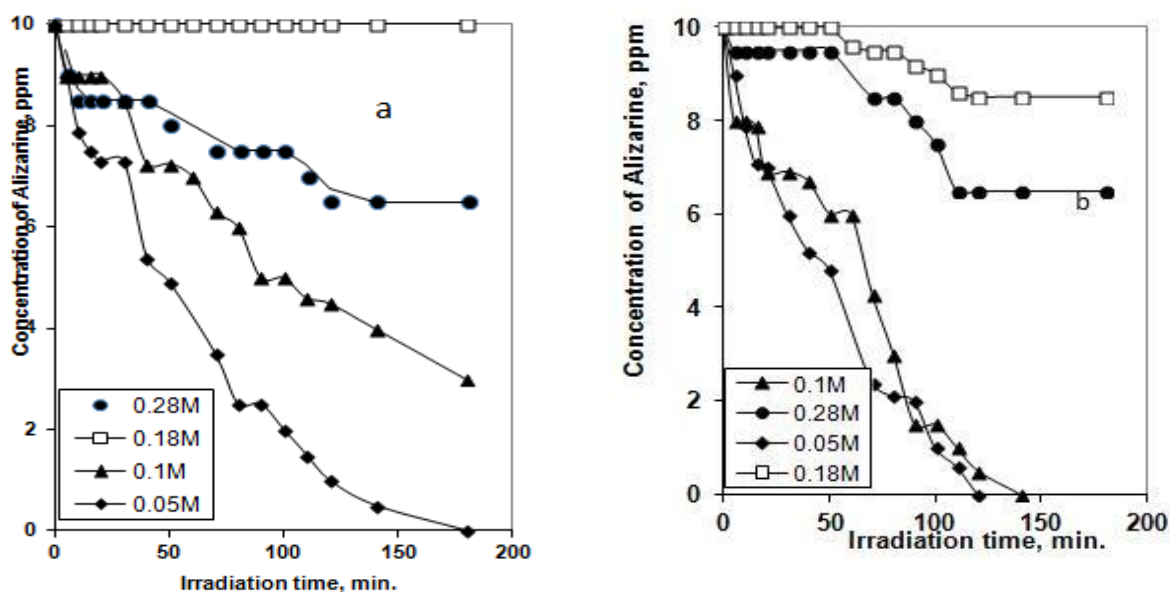


**Figure7 a&b :**  
**Photocatalytic degradation of alizarin yellow by using mesoporous TiO<sub>2</sub> at (a) 400 °C and (b) 600°C.**



## 5. Conclusions

In the present study the photocatalytic degradation of alizarin yellow by TiO<sub>2</sub> nanoparticles, synthesized under different concentrations of silicotungstic acid and calcination temperatures by sol-gel process, was investigated. The correlation between physical properties and photocatalytic activity of TiO<sub>2</sub> nanoparticles according to the different synthesis conditions is as follows:

- As the concentrations of silicotungstic acid increase the crystallinity of the anatase phase is slightly increases and the surface area decreases.
- Alizarin yellow degradation experiments revealed that the photocatalytic activity of TiO<sub>2</sub> nanoparticles was maximized at the calcination temperature of 600 °C.

However, surface area and pore volume of TiO<sub>2</sub> nanoparticles gradually decreases with increasing calcination temperature, indicating that textural properties are not critical for controlling the photocatalytic activity of TiO<sub>2</sub> nanoparticles. The trend is likely due to the combined effect of the anatase crystallinity, showed the highest value at 600 °C and the crystallite size did not excessively increase up to 600 °C.

## References

- Abdel-Azim, S.M., Aboul-Gheit, A. K., Ahmed ,S. M., El-Desouki, D. S.& Abdel-Mottaleb, M. S. A., (2014) Preparation and Application of Mesoporous Nanotitania Photocatalysts Using Different Templates and pH Media, *International Journal of Photoenergy*, Article ID 687597, 11 pages DOI.org/10.1155/2014/687597.
- Anpo, M. & Yamashita, H. (1996), in: Anpo, M. (Ed.), *Surface Photochemistry*, Wiley, Chichester, 117–164.
- Asuha, S., Zhou, X.G. & Zhao, S. (2010), “Adsorption of methyl orange and Cr(VI) on mesoporous TiO<sub>2</sub> prepared by hydrothermal method”, *Journal of Hazardous Materials* **181**, 204–210, DOI: 10.1016/j.jhazmat.2010.04.117.
- Balachandran, U. & Eror, N.G. (1982), “Raman spectra of titanium dioxide”, *J. Solid State Chem.* **42**, 276–282, DOI: 10.1016/0022-4596(82)90006-8.
- Bauer, A., Chevallier, L., Hui, R., Cavaliere, S., Zhang, J., Jones, D. & Rozi ère, J. (2012), “Synthesis and characterization of Nb-TiO<sub>2</sub> mesoporous microsphere and nanofiber supported Pt catalysts for high temperature PEM fuel cells”, *Electrochimica Acta* **77**, 1–7, DOI: 10.1016/j.electacta.2012.04.028.
- Boujday, S., W ünsch, F., Portes, P., Bocquet, J.-F. & Colbeau-Justin, C. (2004), “Photocatalytic and Electronic Properties of TiO<sub>2</sub> Powders Elaborated by Sol-gel route and supercritical drying”, *Solar Energy Materials and Solar Cells* **83**, 421–433, DOI: 10.1016/j.solmat.2004.02.035.
- Cao, T., Li, Y., Wang, C., Shao, C. & Liu, Y. (2011), “One-step Nonaqueous Synthesis of Pure Phase TiO<sub>2</sub> Nanocrystals from TiCl<sub>4</sub> in Butanol and Their Photocatalytic Properties”, *Journal of Nanomaterials* , Article ID 267415, doi:10.1155/2011/267415.
- Chen, C.-Y., Cheng, M.-C. & Chen, A.-H. (2012), “Photocatalytic decolorization of Remazol Black 5 and Remazol Brilliant Orange 3R by mesoporous TiO<sub>2</sub>”, *Journal of Environmental Management* **102**,125-133, DOI: 10.1016/j.jenvman.2012.02.024.
- Chevallier, L., Bauer, A., Cavaliere, S., Hui, R., Rozi ère, J. & Jones, D.J. (2012), “Mesoporous Nanostructured Nb-Doped Titanium Dioxide Microsphere Catalyst Supports for PEM Fuel Cell Electrodes”, *ACS Appl. Mater. Interfaces* **4**, 1752-1759. DOI: 10.1021/am300002j.
- Chong, M.N., Jin, B., Chow, C.W.K. & Saint, C. (2010), “Recent Developments in Photocatalytic Water Treatment Technology: A review”, *Water Research* **44**, 2997–3027, DOI: 10.1016/j.watres.2010.02.039.
- Chung, K.-T. & Stevens Jr, S.E. (1993), “Degradation azo dyes by environmental microorganisms and helminths”, *Environ. Toxicol. Chem.* **12**, 2121–2132, DOI: 10.1002/etc.5620121120.
- Di, K., Zhu, Y., Yang, X. & Li, C. (2006), “Electrorheological behavior of urea-doped mesoporous TiO<sub>2</sub> suspensions”, *Colloids and Surfaces A-Physicochem. Eng. Aspects* **280**, 71–75, DOI: 10.1016/j.colsurfa.2006.01.032.
- Ding, Z., Lu, G.Q. & Greenfield, P.F. (2000), “Role of the Crystallite Phase of TiO<sub>2</sub> in Heterogeneous Photocatalysis for Phenol Oxidation in Water”, *J. Phys. Chem. B* **104**, 4815–4820, DOI: 10.1021/jp993819b.
- Duan, Y., Fu, N., Fang, Y., Li, X., Liu, Q., Zhou, X. & Lin, Y. (2013), “Synthesis and formation mechanism of mesoporous TiO<sub>2</sub> microspheres for scattering layer in dye-sensitized solar cells”, *Electrochimica Acta* **113**, 109–116, DOI:

10.1016/j.electacta.2013.09.057.

Dumont, J., Jossé R., Lambert, C., Anthérieu, S., Le Hegarat, L., Aninat, C., Robin, M., Guguen-Guillouzo, C. & Guillouzo, A. (2010), "Differential toxicity of hetero- cyclic aromatic amines and their mixture in metabolically competent HepaRG cells", *Toxicol. Appl. Pharmacol* **245**, 256–263, DOI: 10.1016/j.taap.2010.03.008.

Faisal, M., Ismail, A.A., Harraz, F.A., Bouzid, H., Al-Sayari, S.A. & Al-Hajry, A. (2014), "Mesoporous TiO<sub>2</sub> based optical sensor for highly sensitive and selective detection and preconcentration of Bi(III) ions", *Chemical Engineering Journal* **243**, 509–516, DOI: 10.1016/j.cej.2014.01.028.

Fox, M.A. & Dulay, M.T. (1993), "Heterogeneous photocatalysis", *Chem. Rev.* **93**, 341–357, DOI: 10.1021/cr00017a016.

Fu, Z., Zhang, Y. & Wang, X. (2011), "Textiles wastewater treatment using anoxic filter bed and biological wriggle bed-ozone biological aerated filter", *Bioresour. Technol.* **102**, 3748–3753, doi: 10.1016/j.biortech.2010.12.002.

Fujishima, A., Rao, T.N. & Tryk, D.A. (2000), "Intermolecular and Supramolecular Electron Transfer Processes of Fullerene-Prophyrin/phthalocyanine Systems", *Journal of Photochemistry and Photobiology C* **1**, 1–21.

Gao, L., Li, X., Hu, H., Li, G., Liu, H. & Yu, Y. (2014), "TiO<sub>2</sub> mesoporous microspheres with nanorod structure: facile synthesis and superior electrochemical performance", *Electrochimica Acta* **120**, 231–239, DOI: 10.1016/j.electacta.2013.12.020.

Gopal, M., Moberly Chan, W.J. & De Jonghe, L.C. (1997), "Room Temperature Synthesis of Crystalline Metal Oxides", *Journal of Materials Science* **32**, 6001–6008, DOI: 10.1023/A:1018671212890.

Grosso, D., Soler-Illia, G.J.de A.A., Crepaldi, E.L., Cagnol, F., Sinturel, C., Bourgeois, A., Brunet-Bruneau, A., Amenitsch, H., Albouy, P.A. & Sanchez, C. (2003), "Highly Porous TiO<sub>2</sub> anatase Optical Thin Films with Cubic Mesostructure Stabilized at 700 °C", *Chem. Mater.* **15**, 4562–4570, DOI: 10.1021/cm031060h.

Guo, J., Zhou, J., Wang, D., Xiang, X., Yu, H., Tian, C. & Song, Z. (2006), "Correlation of anaerobic biodegradability and the electrochemical characteristic of azo dyes", *Biodegradation* **17**, 341–346, DOI: 10.1007/s10532-005-9003-0.

Guo, N., Liang, Y., Lan, S., Liu, L., Ji, G., Gan, S., Zou, H. & Xu, X. (2014), "Uniform TiO<sub>2</sub>-SiO<sub>2</sub> hollow nanospheres: Synthesis, Characterization and enhanced adsorption-photodegradation of azo dyes and phenol", *Applied Surface Science* **305**, 562-574, DOI: 10.1016/j.apsusc.2014.03.136.

Hagfeldt, A. & Graetzel, M. (1995), "Light-Induced Redox Reactions in Nanocrystalline Systems", *Chem. Rev.* **95**, 49–68, DOI: 10.1021/cr00033a003.

Han, Y., Kim, H.-S. & Kim, H. (2012), "Relationship between Synthesis Conditions and Photocatalytic Activity of Nanocrystalline TiO<sub>2</sub>", *Journal of Nanomaterials* 2012, Article ID 427453, DOI: 10.1155/2012/427453.

Heller, A. (1995), "Chemistry and Applications of Photocatalytic Oxidation of Thin Organic Films", *Chem. Res.* **28**, 503–508, DOI: 10.1021/ar00060a006.

Hoffmann, M.R., Martin, S.T., Choi, W. & Bahnemann, D.W. (1995), "Environmental Applications of Semiconductor Photocatalysis", *Chem. Rev.* **95**, 69–96, DOI: 10.1021/cr00033a004.

Hu, J. & Wang, J. (2007), "Degradation of chlorophenols in aqueous solution by  $\gamma$ - radiation", *Radiat., Phys.Chem.* **76**, 1489–1492, DOI: 10.1016/j.radphyschem.2007.02.058.m.

Ilinoiu, E.C., Pode, R., Manea, F., Colar, L.A., Jakab, A., Orha, C., Ratiu, C., Lazau, C. & Sfarloag, P. (2013), "Photocatalytic activity of a nitrogen-doped TiO<sub>2</sub> modified zeolite in the degradation of Reactive Yellow 125 azo dye", *Journal of the Taiwan Institute of Chemical Engineers* **44**, 270–278, DOI: 10.1016/j.jtice.2012.09.006.

IUPAC reporting physisorption data for gas/solid system (1985), *Pure and Applied Chemistry* **57**, 1723.

Janik, M.J., Campbell, K.A., Bardin, B.B., Davis, R.J. & Neurock, M. (2003), "A computational and experimental study of anhydrous phosphotungstic acid and its interaction with water molecules", *Appl. Catal. A: General* **256**, 51-68, DOI: 10.1016/S0926-860X(03)00388-0.

Janik, M.J., Davis, R.J. & Neurock, M. (2005), "Anhydrous and water-assisted proton mobility in phosphotungstic acid", *J. Am. Chem. Soc.* **127**, 5238–5245, DOI: 10.1021/ja042742o.

Jantawasu, P., Sreethawong, T. & Chavadej, S. (2009), "Photocatalytic activity of nanocrystalline mesoporous-assembled TiO<sub>2</sub> photocatalyst for degradation of Methyl Orange monoazo dye in aqueous wastewater", *Chem. Eng. J.* **155**, 223 - 233, DOI: 10.1016/j.cej.2009.07.036.

Jianlong, W. & Jiazhuo, W. (2007), "Application of radiation technology to sewage sludge processing: a review", *J. Hazard. Mater.* **143**, 2–7, DOI: 10.1016/j.jhazmat.2007.01.027.

Jiao, X., Yu, H., Kong, Q., Luo, Y., Chen, Q. & Qu, J. (2014), "Theoretical mechanistic studies on the degradation of alizarin yellow R initiated by hydroxyl radical", *Journal of Physical Organic Chemistry* **27**, 519–526, DOI: 10.1002/poc.3294.

Kamat, P.V. (1993), "Photochemistry on Nonreactive and Reactive (semiconductor) Surfaces", *Chem. Rev.* **93**, 267–300, DOI: 10.1021/cr00017a013.

Khalil, K.M.S., Baird, T., Zaki, M.I., El-Samahy, A.A. & Awad, A.M. (1998), "Synthesis and Characterization of Catalytic Titanias via Hydrolysis of Titanium (IV) Isopropoxide", *Colloids and Surfaces A Physicochemical and Engineering Aspects* **132**, 31-44, DOI: 10.1016/S0927-7757(97)00156-8.

Kim, H.-J., Jeon, J.-D. & Kwak, S.-Y. (2013), "Highly dispersed mesoporous TiO<sub>2</sub> spheres via acid treatment and its application for dye-sensitized solar cells", *Powder Technology* **243**, 130–138, DOI: 10.1016/j.powtec.2013.02.036.

- Lakshmi, B.B., Patrisi, C.J. & Martin, C.R. (1997), "Sol-gel template synthesis of semiconductor oxide micro- and nanostructures", *Chem. Mater.* **9**, 2544–2550, DOI: 10.1021/cm970268y.
- Li, C., Luo, Y., Guo, X., Li, D., Mi, J., Sǿ L., Hald, P., Meng, Q. & Iversen, B.-B. (2012), "Mesoporous TiO<sub>2</sub> aggregate photoanode with high specific surface area and strong light scattering for dye-sensitized solar cells", *Journal of Solid State Chemistry* **196**, 504–510, DOI: 10.1016/j.jssc.2012.07.014.
- Li, X-Y, Chen, L-H., Rooke, J-C., Deng, Z., Hu, Z-Y., Wang, S-Z., Wang, L., Li, Y., Krief, A. & Su, B-L. (2013), "Mesoporous titanium Dioxide (TiO<sub>2</sub>) with hierarchically 3D dendrimeric architectures: Formation mechanism and highly enhanced photocatalytic activity", *Journal of colloid and interface Science* **394**, 252-262, doi: 10.1016/j.jcis.2012.11.014.
- Li, Y., Li, X., Li, J. & Yin, J. (2006), "Photocatalytic Degradation of Methyl Orange by TiO<sub>2</sub>-Coated Activated Carbon and Kinetic Study", *Water Research* **40**, 1119–1126, DOI: 10.1016/j.watres.2005.12.042.
- Lima, R.O.A., Bazo, A.P., Salvadori, D.M.F., Rech, C.M., Oliveira, D.P. & Umbuzeiro, G.A. (2007), "Mutagenic and carcinogenic potential of a textile azo dye processing plant effluent that impacts a drinking water source", *Mutat. Res. Genet. Toxicol. Environ. Mutag.* **626**, 53–60, DOI: 10.1016/j.mrgentox.2006.08.002.
- Liu, F., Liu, C.-L., Hu, B., Kong, W.-P. & Qi, C.-Z. (2012), "High-temperature hydrothermal synthesis of crystalline mesoporous TiO<sub>2</sub> with superior photo catalytic activities", *Applied Surface Science* **258**, 7448–7454, DOI: 10.1016/j.apsusc.2012.04.059.
- Lodha, B. & Chaudhari, S. (2007), "Optimization of Fenton-biological treatment scheme for the treatment of aqueous dye solutions", *J. Hazard. Mater.* **148**, 459–466, DOI: 10.1016/j.jhazmat.2007.02.061.
- Lučić, M., Milosavljević, N., Radetić, M., Šaponjić, Z., Radoičić, M. & Krušić, M.K. (2014), "The potential application of TiO<sub>2</sub>/hydrogel nanocomposite for removal of various textile azo dyes", *Separation and Purification Technology* **122**, 206–216, DOI: 10.1016/j.seppur.2013.11.002.
- Lv, K., Xiang, Q. & Yu, J. (2011), "Effect of Calcination Temperature on Morphology and Photocatalytic Activity of Anatase TiO<sub>2</sub> Nanosheets with Exposed {001} Facets", *Applied Catalysis B: Environmental* **104**, 275–281, DOI: 10.1016/j.apcatb.2011.03.019.
- Narayanan, L. & Murugesan, T. (2014), "Degradation of Alizarin Yellow R using UV/H<sub>2</sub>O<sub>2</sub> advanced oxidation process", *Environmental Progress & Sustainable Energy* **33**, 482–489, DOI: 10.1002/ep.11816.
- Nerud, F., Baldrian, P., Gabriel, J. & Ogbeifun, D. (2001), "Decolorization of synthetic dyes by the Fenton reagent and the Cu/pyridine/H<sub>2</sub>O<sub>2</sub> system", *Chemosphere* **44**, 957–961, DOI: 10.1016/S0045-6535(00)00482-3.
- Nešić, J., Manojlović, D.D., Anđelković, I., Dojčinović, B.P., Vulić, P.J., Krstić, J. & Roglić, G.M. (2013), "Preparation, characterization and photocatalytic activity of lanthanum and vanadium co-doped mesoporous TiO<sub>2</sub> for azo-dye degradation", *Journal of Molecular Catalysis A: Chemical* **378**, 67–75, DOI: 10.1016/j.molcata.2013.05.018.
- Nikkanen, J.-P., Kanerva, T. & Mäntylä T. (2007), "The Effect of Acidity in Low-Temperature Synthesis of Titanium Dioxide", *Journal of Crystal Growth* **304**, 179–183, DOI: 10.1016/j.jcrysgro.2007.02.012.
- Ollis, D.F. & Al-Ekabi, H. (1993), "Photocatalytic Purification and Treatment of Water and Air", Elsevier science publisher, Amsterdam, 49-65.
- Onsuratoom, S., Chavadej, S. & Sreethawong, T. (2011), "Hydrogen production from water splitting under UV light irradiation over Ag-loaded mesoporous-assembled TiO<sub>2</sub>-ZrO<sub>2</sub> mixed oxide nanocrystal photocatalysts", *International journal of hydrogen energy* **36**, 5246-5261, DOI: 10.1016/j.ijhydene.2011.01.176.
- Park, S.-B., Chung, I. J., Woo, J. W., Kim, T. H., Li, Z., Jin, M., Lee, D. J. & Kim, J. M. (2014), "Improvement of dye-sensitized solar cell performance through infiltration of TiO<sub>2</sub> nanoparticles between mesoporous TiO<sub>2</sub> particles", *Materials Research Bulletin* xx xxx–xxx, DOI: 10.1016/j.materresbull.2014.04.062.
- Pelizzetti, E. & Serpone, N. (1989), "Photocatalysis: Fundamentals and Applications", Wiley, New York. ISBN-10: 0471626031. ISBN-10: 0471626031.
- Phonthammachai, N., Chairassameewong, T., Gualri, E., Jamieson, A.M. & Wongkasemjit, S. (2003), "Structural and Rheological aspect of Mesoporous Nanocrystalline TiO<sub>2</sub> Synthesized via Sol-gel Process", *Micropor. Mesopor. Mater.* **66**, 261-271, DOI: 10.1016/j.micromeso.2003.09.017.
- Qian, S., Caiyun, J., Yuping, W., Weiben, Y. & Chun, Y. (2013), "Preparation and characterization of PVA - I complex doped, mesoporous TiO<sub>2</sub> by hydrothermal method", *Applied Surface Science* **273**, 769–775. DOI: 10.1016/j.apsusc.2013.02.132.
- Sakatani, Y., Grosso, D., Nicole, L., Boissière, C., Soler-Illia, G.J.de A.A. & Sanchez, C. (2006), "Optimised Photocatalytic Activity of Grid-like mesoporous TiO<sub>2</sub> Films: Effect of Crystallinity, Pore Size Distribution and Pore accessibility", *J. Mater. Chem.* **16**, 77–82, DOI: 10.1039/B512824M.
- Sakulkhaemaruehai, S. & Sreethawong, T. (2011), "Synthesis of mesoporous-assembled TiO<sub>2</sub> nanocrystals by a modified urea-aided sol-gel process and their outstanding photocatalytic H<sub>2</sub> production activity", *International journal of hydrogen energy* **36**, 6553-6559, DOI: 10.1016/j.ijhydene.2011.03.005.
- Sharifuddin, J.H., Jones, M.I. & Patterson, D.A. (2013), "Greener photocatalysts: Hydroxyapatite derived from waste mussel shells for the photocatalytic degradation of a model azo dye wastewater". *Chemical Engineering Research and Design* **91**, 1693-1704, DOI: 10.1016/j.cherd.2013.04.018.
- Sharma, K.K., O'Neill, P., Oakes, J., Batchelor, S.N. & Rao, B.S.M. (2003), "One-electron oxidation and reduction of

- different tautomeric forms of azo dyes: a pulse radiolysis study”, *J. Phys. Chem. A* **107**, 7619–7628, DOI: 10.1021/jp035002v.
- Singh, K. & Arora, S. (2011), “Removal of synthetic textile dyes from wastewaters: a critical review on present treatment technologies”, *Crit. Rev. Environ. Sci. Technol.* **41**, 807–878, DOI: 10.1080/10643380903218376.
- Soler-Illia, G.J.de A.A., Crepaldi, E.L., Grosso, D. & Sanchez, C. (2003), “Block Copolymer–Templated Mesoporous Oxides”, *Curr. Opin. Colloid & Interf. Sci.* **8**, 109–126.
- Soler-Illia, G.J.de A.A., Sanchez, C., Lebeau, B. & Patarin, J. (2002), “Chemical strategies to design textured materials: From microporous and mesoporous oxides to nanonetworks and hierarchical structures”, *Chem. Rev.* **102**, 4093–4138, DOI: 10.1021/cr0200062.
- Sreethawong, T., Suzuki, Y. & Yoshikawa, S. (2005), “Synthesis, characterization and photocatalytic activity for hydrogen evolution of nanocrystalline mesoporous titania prepared by surfactant-assisted templating sol–gel process”, *J. Solid State Chem.* **178**, 329–338, DOI: 10.1016/j.jssc.2004.11.014.
- Sudarjanto, G., Keller-Lehmann, B. & Keller, J. (2006), “Optimization of integrated chemical–biological degradation of a reactive azo dye using response surface methodology”, *J. Hazard. Mater.* **138**, 160–168, DOI: 10.1016/j.jhazmat.2006.05.054.
- Tanev, P.T. & Pinnavaia, T.J. (1995), “A Neutral Templating Route to Mesoporous Molecular Sieves”, *Science* **267**, 865–867, DOI: 10.1126/science.267.5199.865.
- Tantak., N.P. & Chaudhari, S. (2006), “Degradation of azo dyes by sequential Fenton’s oxidation and aerobic biological treatment”, *J. Hazard. Mater.* **136**, 698–705, DOI: 10.1016/j.jhazmat.2005.12.049.
- Tian, G., Fu, H., Jing, L. & Tian, C. (2009), “Synthesis and photocatalytic activity of stable nanocrystalline TiO<sub>2</sub> with high crystallinity and large surface area”, *Journal of Hazardous Materials* **161**, 1122–1130, DOI: 10.1016/j.jhazmat.2008.04.065.
- Ting, T.-M. & Jamaludin, N. (2008), “Decolorization and decomposition of organic pollutants for reactive and disperse dyes using electron beam technology: effect of the concentrations of pollutants and irradiation dose”, *Chemosphere* **73**, 76–80, DOI: 10.1016/j.chemosphere.2008.05.007.
- Topkaya, E., Konyar, M., Yatmaz, H.C. & Öztürk, K. (2014), “Pure ZnO and composite ZnO/TiO<sub>2</sub> Catalyst Plates: A Comparative Study for the Degradation of Azo dye, Pesticide and Antibiotic in Aqueous Solutions”, *Journal of Colloid and interface Science* **430**, 6–11, DOI: 10.1016/j.jcis.2014.05.022.
- Turesky, R.J. (2005), “Interspecies metabolism of heterocyclic aromatic amines and the uncertainties in extrapolation of animal toxicity data for human risk assessment”, *Mol. Nutr. Food Res.* **49**, 101–117, DOI: 10.1002/mnfr.200400076.
- Vahdat, A., Bahrami, S.H., Arami, M. & Motahari, A. (2010), “Decomposition and decoloration of a direct dye by electron beam radiation”, *Radiat. Phys. Chem.* **79**, 33–35, DOI: 10.1016/j.radphyschem.2009.08.012.
- Wang, J. & Xu, L.J. (2012), “Advanced oxidation processes for wastewater treatment: formation of hydroxyl radical and application”, *Crit. Rev. Environ. Sci. Technol.* **42**, 251–325, DOI: 10.1080/10643389.2010.507698.
- Wang, R., Cai, X. & Shen, F. (2014), “TiO<sub>2</sub> hollow microspheres with mesoporous surface: Superior adsorption performance for dye removal”, *Applied Surface Science* **305**, 352–358, DOI: 10.1016/j.apsusc.2014.03.089.
- Wang, W., Lu, C., Ni, Y., Peng, F. & Xu, Z. (2013), “Enhanced performance of {0 0 1}facets dominated mesoporous TiO<sub>2</sub> photocatalyst composed of high-reactive nanocrystals and mesoporous spheres”, *Applied Surface Science* **265**, 438–442, DOI: 10.1016/j.apsusc.2012.11.025.
- Wojnárovits, L. & Takács, E. (2008), “Irradiation treatment of azo dye containing wastewater: an overview”, *Radiat. Phys. Chem.* **77**, 225–244, DOI: 10.1016/j.radphyschem.2007.05.003.
- Wongkalasin, P., Chavadej, S. & Sreethawong, T. (2011), “Photocatalytic degradation of mixed azo dyes in aqueous wastewater using mesoporous-assembled TiO<sub>2</sub> nanocrystal synthesized by a modified sol–gel process”, *Colloids and Surfaces A: Physicochemical and Engineering Aspects* **384**, 519–528, DOI: 10.1016/j.colsurfa.2011.05.022.
- Xiong, Z., Ma, J., Ng, W.J., Waite, T.D. & Zhao, X.S. (2011), “Silver-modified mesoporous TiO<sub>2</sub> photocatalyst for water Purification”, *Water Research* **45**, 2095–2103, DOI: 10.1016/j.watres.2010.12.019.
- Yu, J., Wang, G., Cheng, B. & Zhou, M. (2007), “Effect of hydrothermal Temperature and Time on the Photocatalytic Activity and Microstructures of Bimodal Mesoporous TiO<sub>2</sub> Powders”, *Applied Catalysis B: Environmental* **69**, 171–180, DOI: 10.1016/j.apcatb.2006.06.022.
- Yu, S., Hu, J. & Wang, J. (2010), “Radiation-induced catalytic degradation of p-nitrophenol (PNP) in the presence of TiO<sub>2</sub> nanoparticles”, *Radiat.Phys.Chem.* **79**, 1039–1046, DOI: 10.1016/j.radphyschem.2010.05.008.
- Zhang, J., Li, M., Feng, Z., Chen, J. & Li, C. (2006), “UV Raman Spectroscopic Study on TiO<sub>2</sub>. 1. Phase Transformation at the Surface and in the Bulk”, *J. Phys. Chem.B* **110**, 927–935, DOI: 10.1021/jp0552473.
- Zhang, X., Zhang, F. & Chan, K.-Y. (2005), “Synthesis of Titania-Silica Mixed Oxide Mesoporous Materials, Characterization and Photocatalytic Properties”, *Applied Catalysis A: General* **284**, 193–198, DOI: 10.1016/j.apcata.2005.01.037.
- Zhao, B., Cai, R., Jiang, S., Sha, Y. & Shao, Z. (2012), “Highly flexible self-standing film electrode composed of mesoporous rutile TiO<sub>2</sub>/C nanofibers for lithium-ion batteries”, *Electrochimica Acta* **85**, 636–643, DOI: 10.1016/j.electacta.2012.08.126.
- Zhou, R., Zhang, Q., Uchaker, E., Yang, L., Yin, N., Chen, Y., Yin, M. & Cao, G. (2014), “Photoanodes with mesoporous

---

TiO<sub>2</sub> beads and nanoparticles for enhanced performance of CdS/CdSe quantum dot co-sensitized solar cells”, *Electrochimica Acta* 135, 284-292, DOI: 10.1016/j.electacta.2014.05.021.

Zhu, L., Liu, K., Li, H., Sun, Y. & Qiu, M. (2013), “Solvothermal synthesis of mesoporous TiO<sub>2</sub> microspheres and their excellent photocatalytic performance under simulated sunlight irradiation”, *Solid state Sciences* **20**, 8-14, DOI: 10.1016/j.solidstatedsciences.2013.02.026.